CFSRC COLLOQUIUM

Proceedings of the Cold-Formed Steel Research Consortium Colloquium
20-22 October 2020 (cfsrc.org)

Post-elastic Capacity of Thin-walled Cold-formed Steel Members

Dan Dubina[1], Viorel Ungureanu[2], Maria Kotełko [3]

Abstract

The paper presents the possibility to apply the local plastic mechanisms to characterize the ultimate strength of thin-walled cold-formed steel members subjected to eccentric compression. In previous papers [13], [14], [18], the authors have shown that, for compression or bending, the failure of such sections modelled by localized plastic mechanisms characterize better the behaviour of thin-walled cold-formed short members in Ultimate Limit State. These models are consistent with the real failure mechanism of short members and were confirmed both by experimental tests and advanced elastic-plastic FEM analyses. Selected results from these studies are summarized in Chapter 2 of the paper. The main aim of the actual paper concerns the more complex problem of members subjected to combined loadings i.e. compression and bending or eccentric compression. The failure model of slender members in eccentric compression is still an open question. In an attempt to solve this problem, the authors propose a consistent methodology which applies the General Method of EN1993 Part 1-1, in which the section resistance, prone to bending and compression, is characterized through plastic mechanism failure models.

1. General

The EN 1993-1-1 [1] code defines four classes of cross-sections for steel structural elements. Thin-walled cold-formed steel structures are usually made of Class 4 section members (at the limit, they might be of Class 3). These sections are prematurely prone to local or distortional buckling, while for members of intermediate lengths (members with a reduce slenderness, $\bar{\lambda}$, in the range 0.7-1.5), the interactive buckling is present. To calculate the effective properties of the cross-section due to local buckling, Winter formula for the effective width is used in the major design code provisions (EN1993-1-3:2006 [2], AISI S100-16 [3], AS/NZS 4600:2018 [4]). Moreover, Part 2 of DIN 18800 allows to calculate the load-carrying capacity of cross-sections with the help of the effective width method according to the elastic-plastic procedure.

In the last decades, intensive progress in studying the individual and interactive buckling modes was done due to the development of specific numerical methods. The Generalized Beam Theory (GBT) [5, 6, 7] has been developed extensively. Alternatively, the constrained Finite Strip Method (cFSM) [8] has been developed.

The interactive buckling of thin-walled cold-formed steel slender members is covered by the design codes too [2, 3, 4]. Moreover, Part 1.1 of EN1993 [1] proposes the General Method to be used where the classic methods given in 6.3.1, 6.3.2 and 6.3.3 of the code do not apply.

Direct Strength Method, proposed by Schafer [9], replaces the “effective width” concept with the “effective stress” one. The method explicitly incorporates local or distortional and Euler buckling and does not require calculations of the effective properties. DSM is an alternative to the “effective width” method and it has been adopted in 2004 as design method in Appendix 1 to the *North American Specification for the Design of Cold-Formed Steel Structural Members* [3].

An alternative for studying the interactive buckling is the ECBL (i.e. Erosion of Critical Bifurcation Load) approach [10], enabling to evaluate experimentally or numerically the theoretical erosion of critical load into the interactive buckling range. Practically, ECBL can be used to calibrate the α-imperfection factor in Ayrton-Perry interactive equation of EN 1993-1-3 [11].

Cold-formed steel sections are traditionally considered with no plastic capacity, and consequently non-ductile, mainly due to wall slenderness involving local instability phenomena. However, although they do not have enough plastic rotation capacity to form plastic hinges, they fail through local plastic mechanisms. Based on this real model,

[1] Professor, Department of Steel Structures and Structural Mechanics, Politehnica University of Timisoara / Laboratory of Steel Structures, Romanian Academy - Timisoara Branch, dan.dubina@upt.ro
[2] Professor, Department of Steel Structures and Structural Mechanics, Politehnica University of Timisoara / Laboratory of Steel Structures, Romanian Academy - Timisoara Branch, viorel.ungureanu@upt.ro
[3] Professor, Department of Strength of Materials, Łodz University of Technology, maria.kotelko@p.lodz.pl

of the behaviour of thin-walled stub columns and short beams, Ungureanu & Dubina [12] used the ECBL approach to express the plastic-elastic interactive buckling of thin-walled members. The main problem of this approach is to evaluate properly the *plastic* strength of thin-walled members [12, 13], via the local plastic mechanism theory and after, the erosion of critical load into the *"plastic-elastic coupling range"*.

2. Plastic mechanisms for members in compression or in bending

In the case of thin-walled cold-formed sections, multiple local buckling modes may occur simultaneously under the same critical load. For a long member, multiple local buckling modes, may interact with each other and give rise to an unstable post-critical behaviour called "localisation of the buckling pattern". The localised buckling mode is, in fact, an interactive or coupled mode. This is a "first" iteration, which may occur before the overall buckling mode of the member. The "second" interaction, between the localised buckling mode and the overall one, is really dangerous because it is accompanied by a very strong erosion of critical bifurcation load [12]. When localisation of buckling patterns occurs, then the member post-buckling behaviour is characterised by large local displacements, in the inelastic range, producing plastic folding of walls, and the member falls into a plastic mechanism.

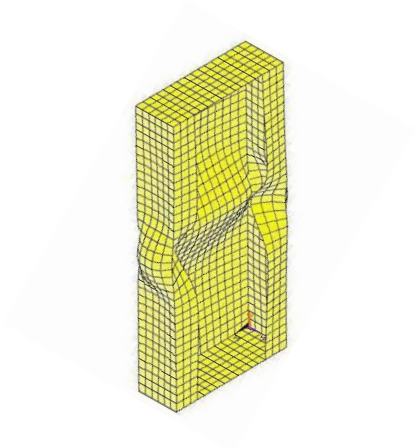

(a) members in compression [12]

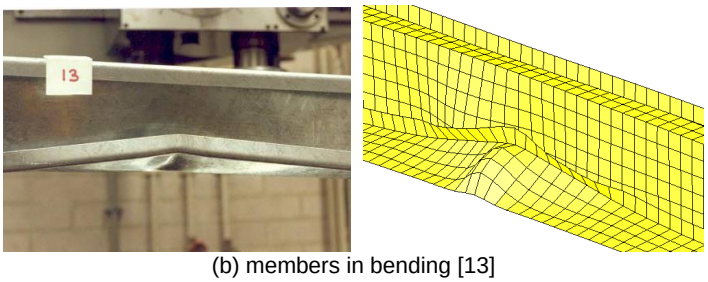

(b) members in bending [13]

Figure1: Numerical and experimental evidence of plastic mechanism failure

This kind of behaviour is specific for cold-formed steel stub columns/short beams and is confirmed both by tests and numerical simulations. Figure 1 provides numerical and experimental evidence of plastic mechanism failure of such sections in compression or in bending.

There are two major classes of plastic mechanisms i.e. true mechanism and quasi-mechanism. A true mechanism is one which is developed from the original thin-walled member by folding the individual plates along the plastic hinge lines. A quasi-mechanism is one which in some regions of the individual plates of the structure is deformed by yielding allowing the plasticized zones to deflect. The mechanism type depends on the yield strength of steel, *b/t* slenderness ratio and the magnitude of initial geometrical imperfections of component walls of the thin-walled steel member. A database for plastic mechanisms for thin-walled cold-formed steel members in compression and bending has been presented in detail in [14].

The main target is to correctly identify the type of plastic mechanism to be used in the analysis (true or quasi-mechanism). In fact, when local buckling firstly appears, it always will develop a localization of buckling patterns which changes into a local plastic mechanism when the member fails (see Figure 2). Therefore, the local plastic mechanism model naturally describes the stub column or short beam behaviour, which is not the case of effective width model. The intersection of the elastic curve and the rigid-plastic one can be used to estimate the ultimate strength of a thin-walled element, considering or not the initial imperfections.

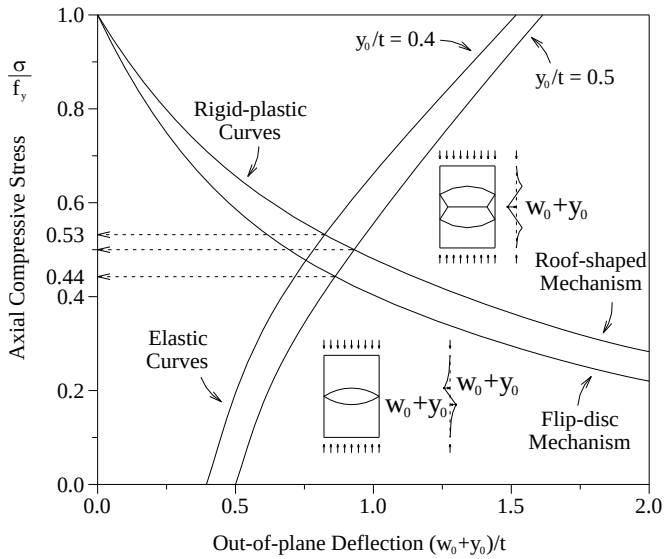

Figure 2: Elastic and rigid-plastic curves for compression plates [15]

Figure 3 shows the local plastic mechanisms available for plain and lipped channel sections in compression, while Figure 4 shows the local plastic mechanisms used for plain and lipped channel sections in bending.

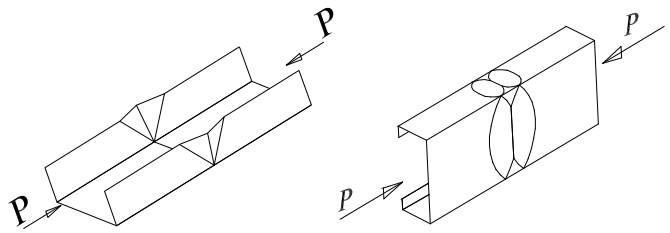

Figure 3: Local plastic mechanisms for a plain and lipped channel in compression

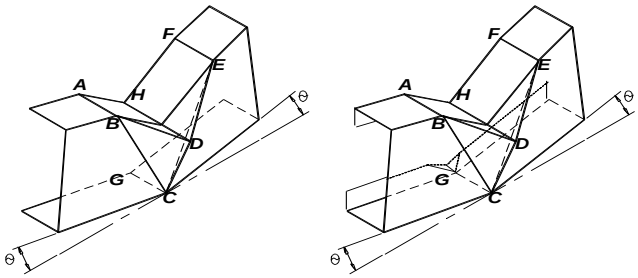

Figure 4: Local plastic mechanisms for a plain and lipped channel in bending

In case of members in compression, Figure 5 presents the $ECBL_{pl-el}$ results [13], compared with those from FEM elastic-plastic analysis, the ECBL elastic-elastic, $ECBL_{el-el}$, and experimental tests performed by Batista [16].

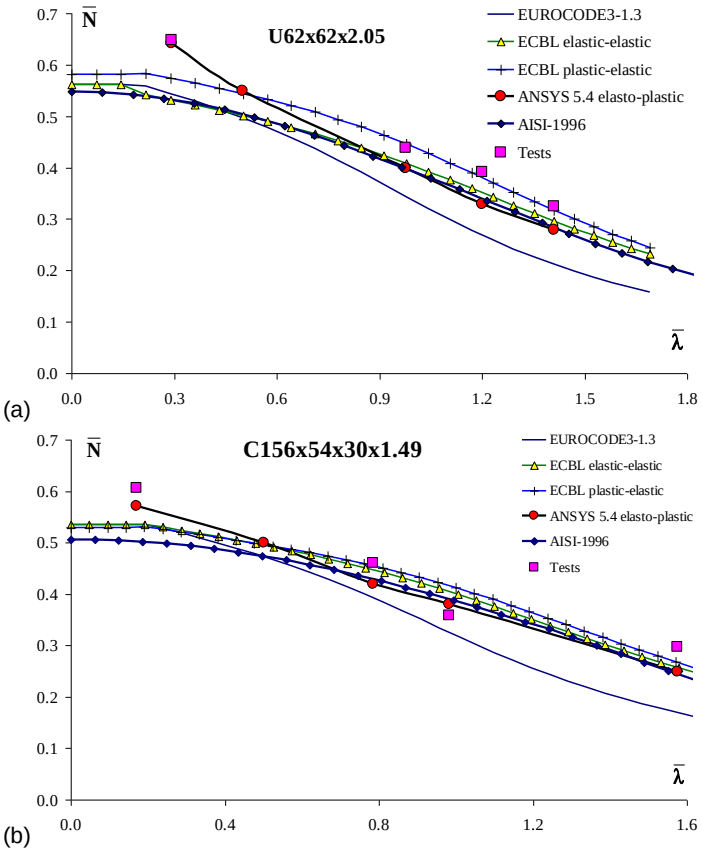

Figure 5: Numerical/Experimental comparison for members in compression [13]

EN1993-Part.1.3 [2] and AISI [3] results are also included in this comparison. It is easy to see the quality of $ECBL_{pl-el}$ results are excellent, particularly in the interactive zone, e.g. $0.4<\bar{\lambda}<1.6$.

In the case of slender beams, experimental data performed by Lovell [17] were used to compare the $ECBL_{pl-el}$ and $ECBL_{el-el}$ results with those of EN1993-Part.1.3 [2] and AISI [3] results. Figure 6 shows again that $ECBL_{pl-el}$ model confirms its accuracy [13].

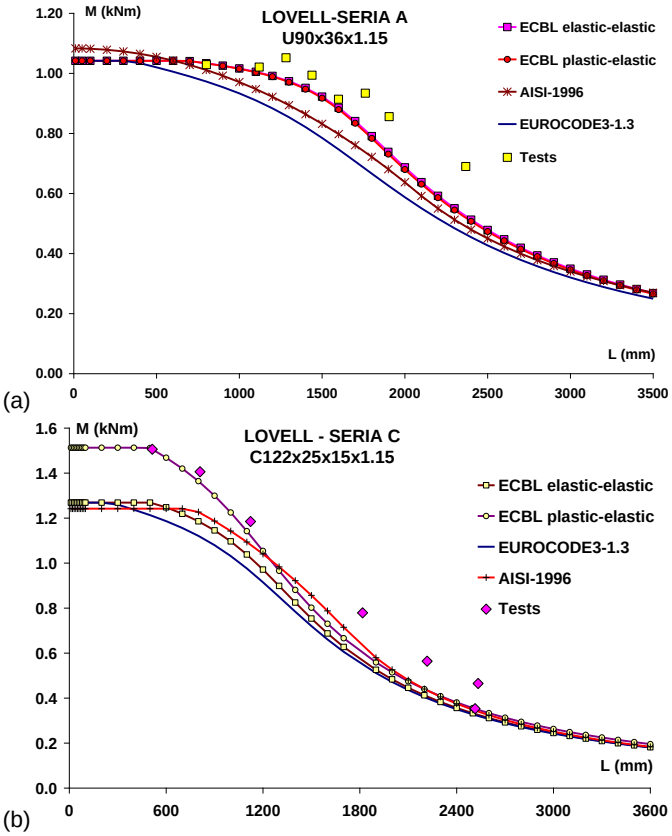

Figure 6: Numerical/Experimental comparison for members in bending [13]

The plastic-elastic interactive model naturally describes the phenomenon of the interactive buckling of thin-walled members. The ECBL plastic-elastic interactive approach, based on the erosion theory of coupled bifurcation, is much more rigorous and understandable than the semi-empirical methods used for the buckling curves in existing design codes.

3. Experimental tests on members in eccentric compression

In the present section, an experimental study on structural behaviour (including post-failure behaviour) of thin-walled cold-formed steel lipped channel section columns subjected to eccentric compression about the minor axis, as shown in

Figure 7 is discussed. The objectives of the study were: determination of the ultimate loads and plastic mechanisms of failure, as well validation and calibration of FE models. The authors, in an accompanying paper [18], developed analytical formulations for collapse plastic mechanisms to characterised the ultimate strength of short lipped channel members subjected to eccentric compression about the minor axis.

3.1 Selection of the specimens

The nominal dimensions of the lipped channel cross-sections under investigation are $a \times b \times c \times t$ = 150×60×20×2 mm with and an internal radius r = 1.5 mm, as shown in Figure 7. The length of the columns was L = 450 mm. The specimens were manufactured on the folding machine.

Since the buckling mode influences on a large extent the failure mode of the compressed bar, firstly, the buckling behaviour of the columns with different eccentricities were investigated. Buckling loads and modes were determined for the large range of eccentricities, from e = -40 mm to e = +40 mm. The analysis was carried out using CUFSM code [8] based on Finite Strip Method.

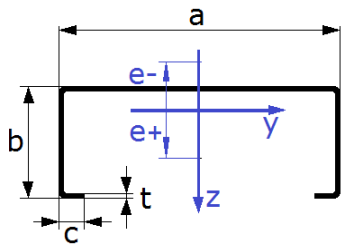

Figure 7: General dimensions of the lipped channel sections

Figure 8 presents the buckling modes and corresponding half-wave lengths of the selected cross-section for two sets of selected eccentricities, i.e. e = ±15 mm and ±40 mm, respectively. It can be observed, for all positive eccentricities up to the smallest negative one, i.e. e = -5 mm distortional buckling mode is dominant, while from the negative eccentricities e = -10 mm to -40 mm changes to local buckling.

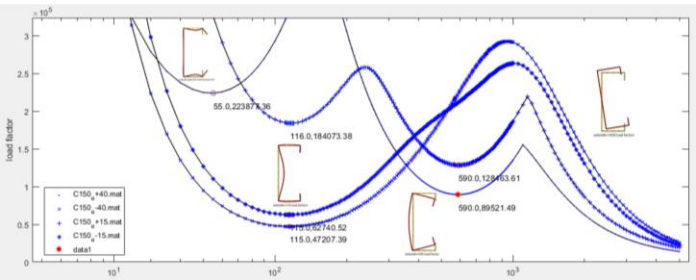

Figure 8: Evolution of the buckling modes for a lipped channel in eccentric compression (e = ±15 mm and ±40 mm)

Consequently, for positive eccentricities, the distortional buckling precedes a typical flange mechanism development, while for negative eccentricities, for which the local buckling mode is observed, a web mechanism develops.

3.2 Experimental test set-up

The idea used in the present research was based on the concept of two rotational cradles installed on the machine. The left side of Figure 9(a) presents the test setup. The cradles bolted to the base plates enable angular motion. Their movable element is equipped with the exchangeable steel plate with grooves to place the short columns in it. As presented in Figure 9(b,c) each groove position induces the centroid and a certain eccentricity. The plates were fastened to cradles, which enabled hinge support on both ends of the column.

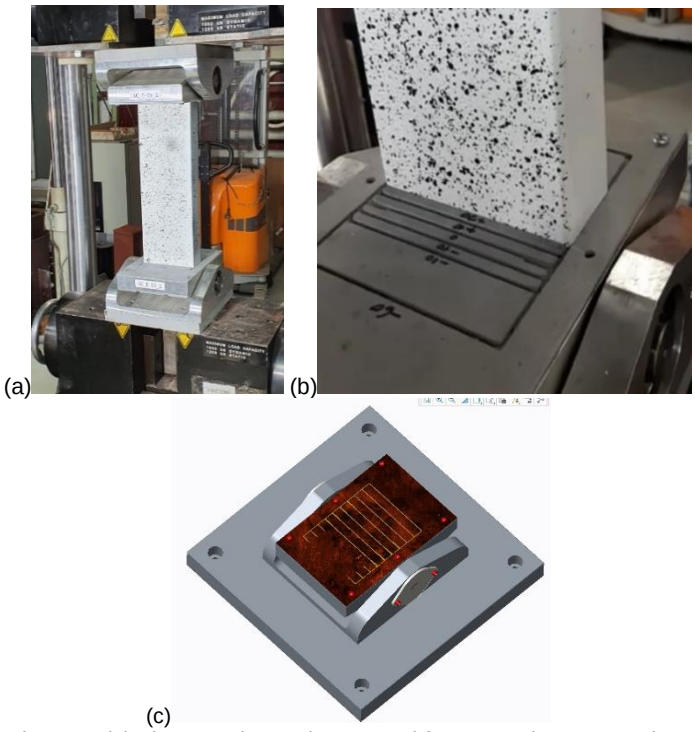

Figure 9: (a) The experimental test stand for eccentric compression; (b) exchangeable steel plate with grooves; (c) groove position to introduce a certain eccentricity related to the centroid

Before testing, the dimensions of all specimens were measured. The working tolerances of the linear dimensions were stated as ±1 mm, whereas the angular ones were about ±1º.

Coupons were cut from the web and flanges of one specimen to perform material tensile tests. Based on those tests, the mean values of material properties were determined (see Figure 10), i.e. yield stress f_y = 417 N/mm^2 and an ultimate strength f_u = 470 N/mm^2, with E = 210000 N/mm^2.

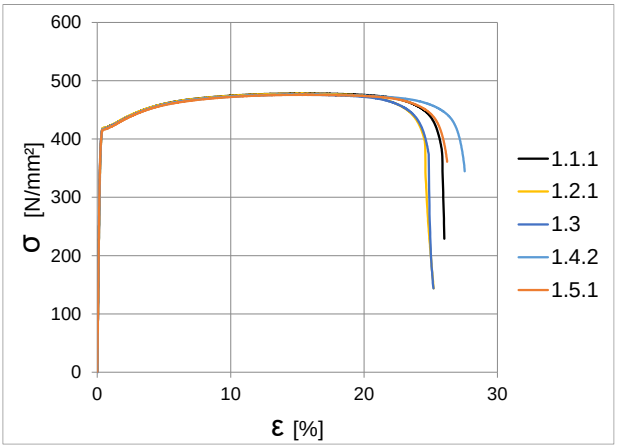

Figure 10: Material behaviour curve for steel specimens

In total, 11 specimens were tested under eccentric load (10 eccentricities and one pure axial load). The following eccentricities were considered: positive and negative of ±5, ±10, ±15, ±20 and ±40 mm.

Specimens were installed in the grip, of on the Instron testing machine (see Figure 9(a)) of loading range Fmax = 1200kN. Eccentric loads were applied to the specimens with the loading velocity of 1 mm/min. Shortening of all specimens was measured in two ways, i.e. (1) using the displacement gauge integrated with the machine crosshead beam and (2) from deformation fields obtained using Digital Image Correlation system (DIC). The DIC system allowed to measure not only shortening of the column but delivered the deformation field maps of the column walls as well.

Figure 11 presents the maximum load for each eccentricity, the associated failure modes and the transition from distortion to local failure with the variation of the eccentricity.

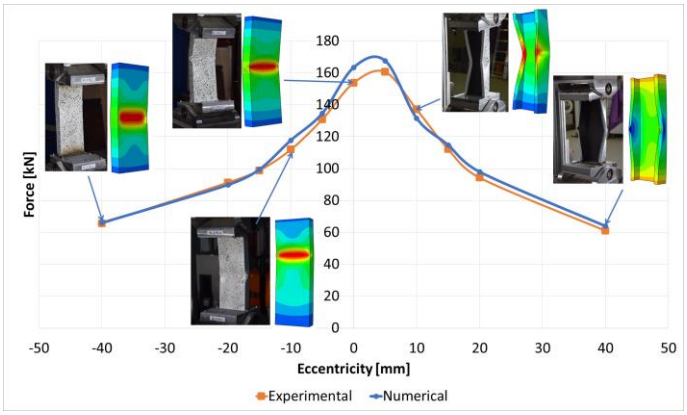

Figure 11: Load vs. eccentricity (experimental vs. numerical)

3.3 Calibration and validation of the numerical model

The numerical models applied to simulate the behaviour of short members in eccentric compression have been built using the commercial FE software ABAQUS/CAE v.6.7.1 [19]. Rectangular 4-node shell elements with reduced integration (S4R) were used to model the thin-walled cold-formed steel members. The chosen mesh size for the shell elements was around 5×5 mm. Static non-linear analyses were carried out in displacement control. Both geometrical and material nonlinearities are included. An isotropic linearly elastic-perfectly plastic constitutive model was considered, with von Mises yielding criterion and associated flow rule. Due to the fabrication process, i.e. folding, it was considered the presence of flexural residual stresses on the cold-formed steel section is negligible.

For numerical simulations, the specimens were considered pinned at one end and simply supported at the other one. For the pinned end support, all three translations together with the rotation along the longitudinal axis of the profile and rotation about the major inertia axis of the cross-section were restrained, while the rotation about minimum inertia axis was free. For the simply supported end, the translations along the cross-section axes, the rotation about the longitudinal axis of the profile and the rotation about the major inertia axis of the cross-section were restrained, while the rotation about the minor inertia axis together and longitudinal translation were free. The analysis was conducted in two steps. The first step consists of a linear buckling analysis (LBA), to find the corresponding buckling modes, affine with the relevant imperfections, i.e. local or distortional. After imposing the initial geometric imperfection (of 2 mm at the level of the cross-section for this particular case), a GMNIA analysis through dynamic explicit method was used to obtain the load-shortening diagrams, considering the corresponding eccentricities.

Figure 11 presents two diagrams (experimental vs. FE) of the maximum loads in terms of applied eccentricities. Details about the deformation obtained, local plastic mechanism development, experiment vs. FE ratio are presented in Figure 12. Ultimate loads decrease significantly with an increase of positive eccentricity and the absolute value of negative eccentricity.

4. General Method of EN1993 Part 1.1 for thin-walled cold-formed members in eccentric compression

The General Method of EN 1993-1.1 may be used where the methods given in 6.3.1, 6.3.2 and 6.3.3 from EN 1993-1.1 do not apply. It allows the verification of the resistance to lateral and lateral-torsional buckling for structural components such as: (1) single members, built-up or not, uniform or not, with complex support conditions or not, or (2) plane frames or subframes composed of such members, which are subject to compression and/or mono-axial bending in the plane, but does not contain rotative plastic hinges.

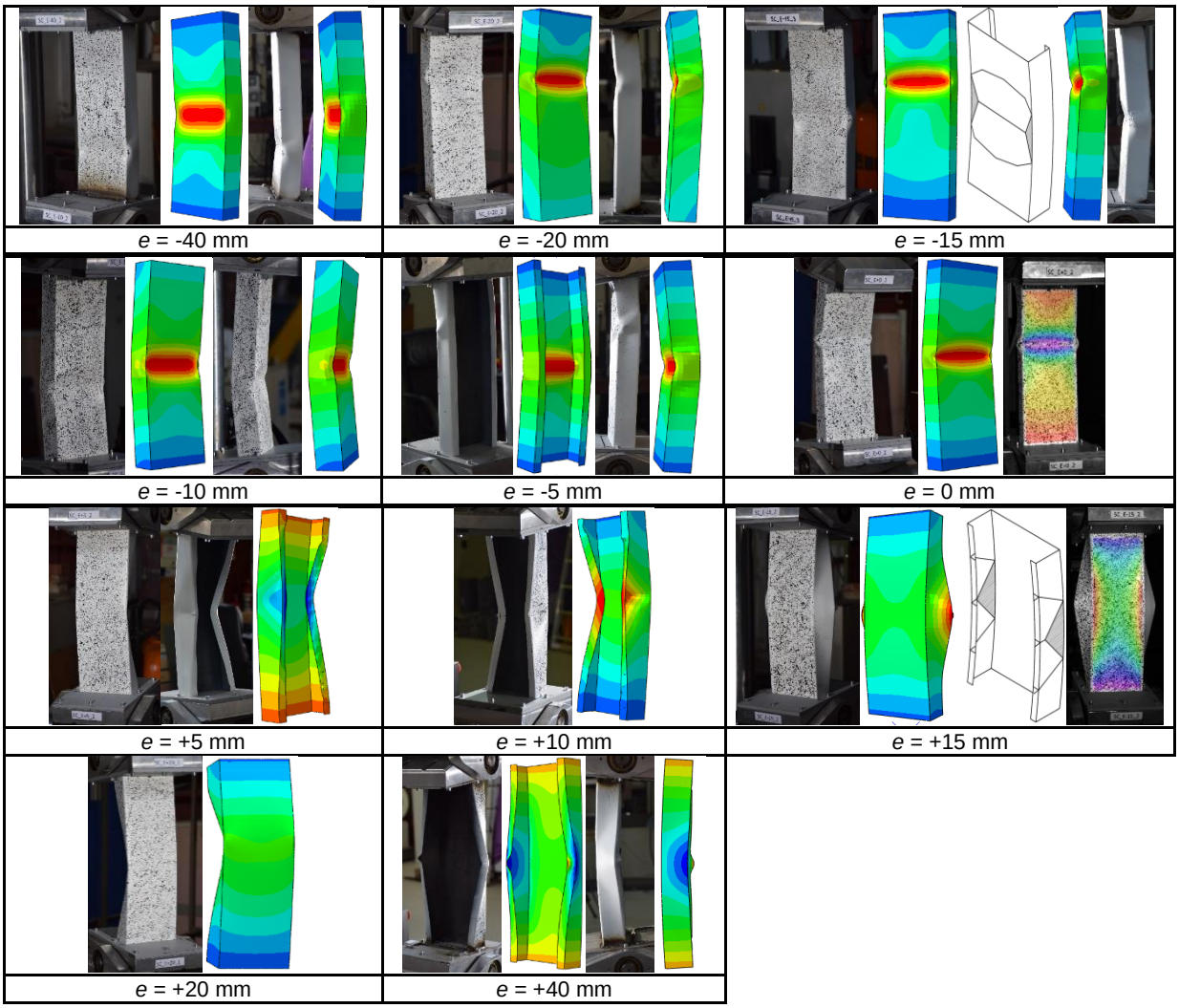

Figure 12: Failure modes vs. eccentricity (experimental vs. numerical)

The overall resistance to out-of-plane buckling for any structural component can be verified by ensuring that:

$$\frac{\chi_{op}\alpha_{ult,k}}{\gamma_{M1}} \geq 1.0 \qquad (1)$$

where

$\alpha_{ult,k}$ is the minimum load amplifier of the design loads to reach the characteristic resistance of the most critical cross-section of the structural component considering its in-plane behaviour without taking lateral or lateral-torsional buckling into account, however accounting for all effects due to in-plane geometrical deformation and imperfections, global and local, where relevant;

χ_{op} is the reduction factor for the non-dimensional slenderness $\bar{\lambda}_{op}$, to take account of lateral and lateral-torsional buckling.

γ_{M1} is the safety coefficient (γ_{M1} = *1*).

The global non-dimensional slenderness $\bar{\lambda}_{op}$ for the structural component should be determined from:

$$\bar{\lambda}_{op} = \sqrt{\frac{\alpha_{ult,k}}{\alpha_{cr,op}}} \qquad (2)$$

where:

$\alpha_{cr.op}$ is the minimum amplifier for the in-plane design loads to reach the elastic critical load of the structural component with regards to lateral or lateral-torsional buckling without accounting for in-plane flexural buckling. In determining $\alpha_{cr.op}$ and $\alpha_{ult.k}$ Finite Element analysis may be used.

The reduction factor χ_{op} may be determined from either of the following methods:

a) the minimum value of

χ for lateral buckling according to 6.3.1;

χ_{LT} for lateral-torsional buckling according to 6.3.2;

each calculated for the global non-dimensional slenderness $\bar{\lambda}_{op}$.

b) a value interpolated between the values χ and χ_{LT} as determined in a) by using the formula for $\alpha_{ult,k}$ corresponding to the critical cross-section. Where $\alpha_{ult,k}$ is determined by the cross-section check, this method leads to:

$$\frac{N_{Ed}}{\chi N_{Rk}/\gamma_{M1}} + \frac{M_{y,Ed}}{\chi_{LT} M_{y,Rk}/\gamma_{M1}} \leq 1 \qquad (3)$$

Two alternatives are proposed for the General Method of EN1993 Part 1.1 for thin-walled cold-formed members in eccentric compression, i.e.

GM1) Eqn. (1) is considered in which: for $\alpha_{ult,k}$ the local plastic mechanism for eccentric compression obtained from the analysis of the short members for the relevant eccentricity is used, while in case of $\alpha_{cr.op}$ the flexural-torsional buckling obtained via CUFSM, as presented in Figure 8, was introduced.

GM2) If $\alpha_{ult,k}$ is determined by the cross-section check, Eqn. (1) of this method leads to:

$$\frac{N_{Ed}}{\chi N_{Rk}/\gamma_{M1}} + \frac{M_{y,Ed}}{\chi_{LT} M_{y,Rk}/\gamma_{M1}} \leq 1$$

where:

- for the term representing compression N_{Rk} uses the effective area and

$$\bar{\lambda} = \sqrt{\frac{N_{Rk}}{N_{cr}}}$$

$$\phi = 0.5\left[1 + \alpha\left(\bar{\lambda} - 0.2\right) + \bar{\lambda}^2\right]$$

$$\chi = \frac{1}{\phi + \sqrt{\phi^2 - \bar{\lambda}^2}} \leq 1$$

- for the term representing compression M_{Rk} uses the effective section modulus and

$$\bar{\lambda}_{LT} = \sqrt{\frac{M_{Rk}}{M_{cr}}}$$

$$\phi_{LT} = 0.5\left[1 + \alpha_{LT}\left(\bar{\lambda}_{LT} - 0.2\right) + \bar{\lambda}_{LT}^2\right]$$

$$\chi_{LT} = \frac{1}{\phi_{LT} + \sqrt{\phi_{LT}^2 - \bar{\lambda}_{LT}^2}} \leq 1$$

in which χ and χ_{LT} will be selected for the corresponding buckling curve.

On the following, to show the accuracy of *General Method* GM1, it will be compared with *General Method* GM2 and results from numerical simulations for two eccentricities, i.e. e = ±15 mm.

The numerical models applied to simulate the behaviour of short and long members in eccentric compression are based on the calibrated numerical models presented in Chapter 3.3, using the same software ABAQUS/CAE v.6.7.1. The GMNIA analyses use the imperfections (local and global) according to Eurocode 3: Design of steel structures - Part 1-14: Design assisted by finite element analysis [20], while for material the experimentally measured σ–ε curves have been used.

Figures 13 and 14 show the good quality results obtained via *General Method GM1.*

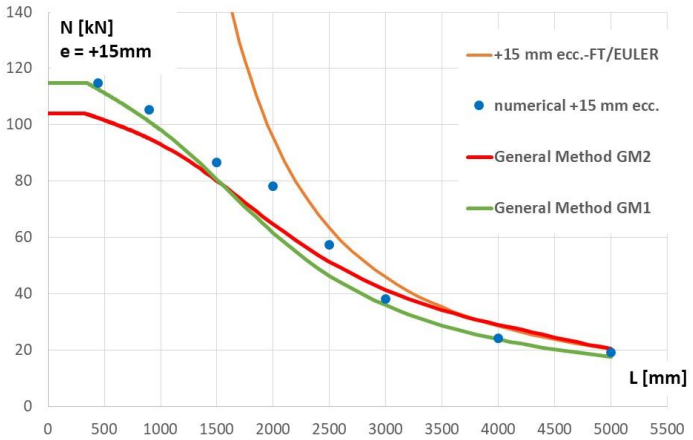

Figure 13: General Method (GM1 and GM2) vs. numerical results for eccentric compression e = +15 mm

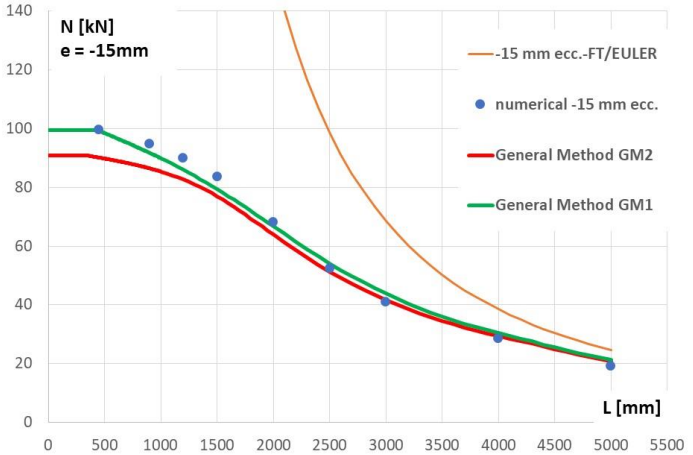

Figure 14: General Method (GM1 and GM2) vs. numerical results for eccentric compression e = -15 mm

5. Conclusions

The local rigid-plastic model describes properly the behavior of thin-walled cold-formed short beams at Ultimate Limit State. This model is consistent with the real failure mechanism of short members and is confirmed both by test results and advanced elastic-plastic FEM analysis.

Both, actual and previous experimental tests and numerical simulations have shown that the effective width approach underestimates the capacity of short members in compression, bending and compression-bending.

The General Method, based on local plastic mechanism, gives very good results and especially in the range of reduced and intermediate slenderness. This method is simple enough to be used in practical design.

Research for a wider range of cross-section as well as various eccentricities (major/minor axes) through experimental and numerical investigations are in progress together with the derivation of appropriate theoretical models of local plastic mechanisms.

6. Acknowledgments

This work was supported by The *Polish - Romanian Joint Research Project: Yield line theory for load-capacity estimation of thin-walled cold-formed steel members under combined loading*, 2019-2021, under the agreement on scientific cooperation between the Polish Academy of Sciences and the Romanian Academy, project *PN-III-CEI-EUREKA-2019/E113493 - CFSExpert - Structural design tool for cold-formed steel structures*, CCCDI - UEFISCDI, Romanian Ministry of Research and Innovation and project 10PFE/2018, *PERFORM-TECH-UPT - The increasing of the institutional performance of the Polytechnic University of Timișoara by strengthening the research, development and technological transfer capacity in the field of "Energy, Environment and Climate Change"*, PNCDI III, Romanian Ministry of Research and Innovation.

References

[1] EN 1993-1-1, Eurocode 3: Design of Steel Structures, Part 1-1: General Rules and Rules for Buildings, Brussels, Belgium, 2005.

[2] EN 1993-1-3, Eurocode 3: Design of Steel Structures, Part 1.3: General Rules, Supplementary Rules for Cold-formed Thin Gauge Members and Sheeting, Brussels, Belgium, 2006.

[3] AISI S100-16, North American Specification for the Design of Cold-Formed Steel Structural Members. Washington, DC, U.S.A., 2016.

[4] AS/NZS 4600:2018, Australian/New Zealand Standard for Cold-formed steel structures, SAI Global Limited, 2018.

[5] Silvestre N, Camotim D., First-order generalised beam theory for arbitrary orthotropic materials, Thin-Walled Structures, 40(9), 755-789, 2002.

[6] Silvestre N, Camotim D., Second-order generalised beam theory for arbitrary orthotropic materials, Thin-Walled Structures, 40(9), 791-820, 2002.

[7] Silvestre N, Camotim D., Nonlinear Generalized Beam Theory for Cold-formed Steel Members, Int. Journal of Structural Stability and Dynamics, 3(4), 461-490, 2003.

[8] Adany S, Schafer BW., A full modal decomposition of thin-walled, single branched open cross-section members via the constrained finite strip method, Journal of Constructional Steel Research, 64, 12–29, 2008.

[9] Schafer BW., Designing Cold-Formed Steel Using the Direct Strength Method, Proceeding of the 18th International Specialty Conference on Cold-Formed Steel Structures, Orlando, Florida, 2006.

[10] Dubina D., The ECBL approach for interactive buckling of thin-walled steel members, Steel & Composite Structures, 1(1), 75−96, 2001.

[11] Dubina D., Ungureanu V., Landolfo R., Design of Cold-formed Steel Structures, Ernst & Sohn, A Wiley Company, Berlin, 2012.

[12] Ungureanu V., Dubina D., Recent research advances on ECBL approach. Part I: Plastic-elastic interactive buckling of cold-formed steel sections, Thin-Walled Structures, 42(2), 177−194, 2004.

[13] Ungureanu V., Dubina D., Post-elastic strength and ductility of cold-formed steel sections, Proceeding of the 4th International Conference on Thin-Walled Structures, Loughborough, UK, 283−290, 2004.

[14] Ungureanu V., Kotełko M., Mania R.J., Dubina, D., Plastic mechanisms database for thin-walled cold-formed steel members in compression and bending, Thin-Walled Structures, 48(10-11), 818-826, 2010.

[15] Mahendran M., Local plastic mechanisms in thin steel plates under in-plane compression, Thin-Walled Structure, 27(3), 245-261, 1997.

[16] Batista E., Essais de profils C et U en acier plies a froid. Rep. No. 157, Universite de Liege, Laboratoire de Stabilite des Constructions, 1986.

[17] Lovell H.M., Lateral buckling of light gauge steel beams. MSc Thesis, University of Salford, UK, 1985.

[18] Ungureanu V., Kotełko M., Karmazyn A., Dubina D., Plastic mechanisms of thin-walled cold-formed steel members in eccentric compression, Thin-Walled Structures, 128, 184-192, 2018.

[19] ABAQUS/Standard Version 6.7-1. “ABAQUS Documentation”, Dassault Systèmes, Providence, RI, USA, 2007 Available at: http://www.simulia.com/.

[20] prEN1993-1-14, Eurocode 3: Design of steel structures - Part 1-14: Design assisted by finite element analysis, Brussels, Belgium, 2020.